

## Near-Ambient-Temperature Dehydrogenative Synthesis of the Amide Bond: Mechanistic Insight and Applications

Sayan Kar,<sup>§</sup> Yinjun Xie,<sup>§</sup> Quan Quan Zhou, Yael Diskin-Posner, Yehoshua Ben-David, and David Milstein\*Cite This: *ACS Catal.* 2021, 11, 7383–7393

Read Online

ACCESS |



Metrics &amp; More



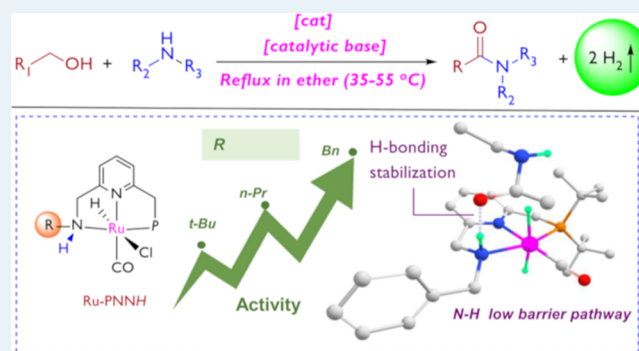
Article Recommendations



Supporting Information

**ABSTRACT:** The current existing methods for the amide bond synthesis *via* acceptorless dehydrogenative coupling of amines and alcohols all require high reaction temperatures for effective catalysis, typically involving reflux in toluene, limiting their potential practical applications. Herein, we report a system for this reaction that proceeds under mild conditions (reflux in diethyl ether, boiling point 34.6 °C) using ruthenium PNNH complexes. The low-temperature activity stems from the ability of Ru–PNNH complexes to activate alcohol and hemiaminals at near-ambient temperatures through the assistance of the terminal N–H proton. Mechanistic studies reveal the presence of an unexpected aldehyde-bound ruthenium species during the reaction, which is also the catalytic resting state. We further utilize the low-temperature activity to synthesize several simple amide bond-containing commercially available pharmaceutical drugs from the corresponding amines and alcohols *via* the dehydrogenative coupling method.

**KEYWORDS:** amides, dehydrogenation, ruthenium pincer, pharmaceuticals, alcohol, amine



## INTRODUCTION

The amide group is one of the most ubiquitous functional groups found in Nature. The formation of the amide bond is a fundamental reaction with important utility in the synthesis of natural compounds, biologically active pharmaceutical drugs, short-chain peptides, industrial chemicals, and polymers such as nylons as well as in devising liquid organic hydrogen carrier systems.<sup>1</sup> Roughly 25% of the currently approved pharmaceutical drugs contain amide groups.<sup>2</sup> The traditional method of facile amide bond synthesis has been the coupling of reactive acid derivatives, such as acid chlorides or anhydrides, with amines, but these methods are poorly tolerated by other nucleophilic functional groups and generate waste. Other methods involve direct coupling of carboxylic acids and amines under milder conditions in the presence of coupling promoters, which also generate significant amounts of waste.<sup>3</sup> In 2005, ACS GCI Pharmaceutical Roundtable reported the “amide bond formation avoiding poor atom economy” as one of the most preferred reactions to develop.<sup>4</sup>

In 2007, our group reported a new, environmentally benign synthesis of the amide bond by acceptorless dehydrogenative coupling of alcohols and amines with H<sub>2</sub> being the sole byproduct of the reaction (Figure 1).<sup>5</sup> The reaction proceeds upon refluxing the alcohol and amine in toluene in the presence of a Ru–PNN catalyst. Since then, many research groups including the groups of Madsen, Crabtree, Hong,

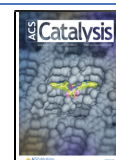
Hazari and Bernskoetter, Prakash, and others have reported efficient catalysts that can catalyze the acceptorless dehydrogenative coupling of alcohols and amines under various conditions.<sup>6</sup> Importantly, first-row transition-metal-based complexes have also been reported for this transformation by the groups of Bernskoetter<sup>6a</sup> (iron) and ours<sup>7</sup> (manganese). Some heterogeneous catalysts are also known to catalyze this transformation.<sup>8</sup>

All the systems mentioned above require a reaction temperature that is generally above 100 °C (typically reflux in toluene), which decreases their practical utility. One of the primary advantages of homogeneous catalysis by well-defined molecular complexes over heterogeneous catalysts is that the activity of the homogeneous complexes can be rationally improved *via* judicious tuning of the ligand framework. The high reaction temperature required for dehydrogenative amide bond formation is presumably due to the difficulty in the hydride abstraction from the reactant and the hemiaminal intermediate by the employed catalysts, en route to the

Received: February 15, 2021

Revised: May 10, 2021

Published: June 7, 2021



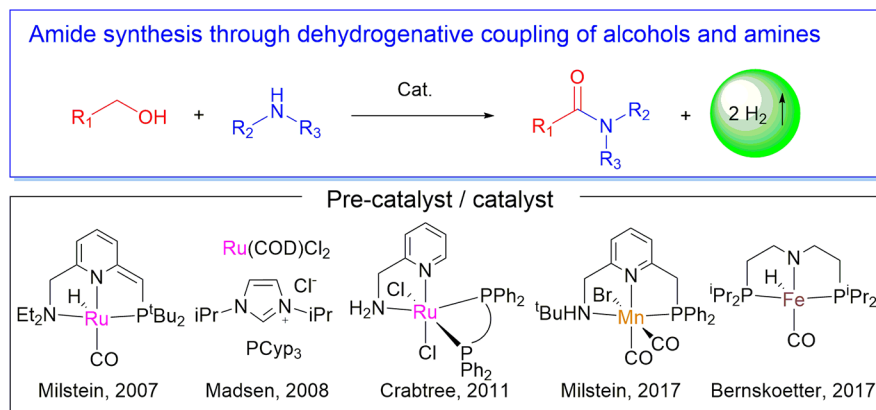
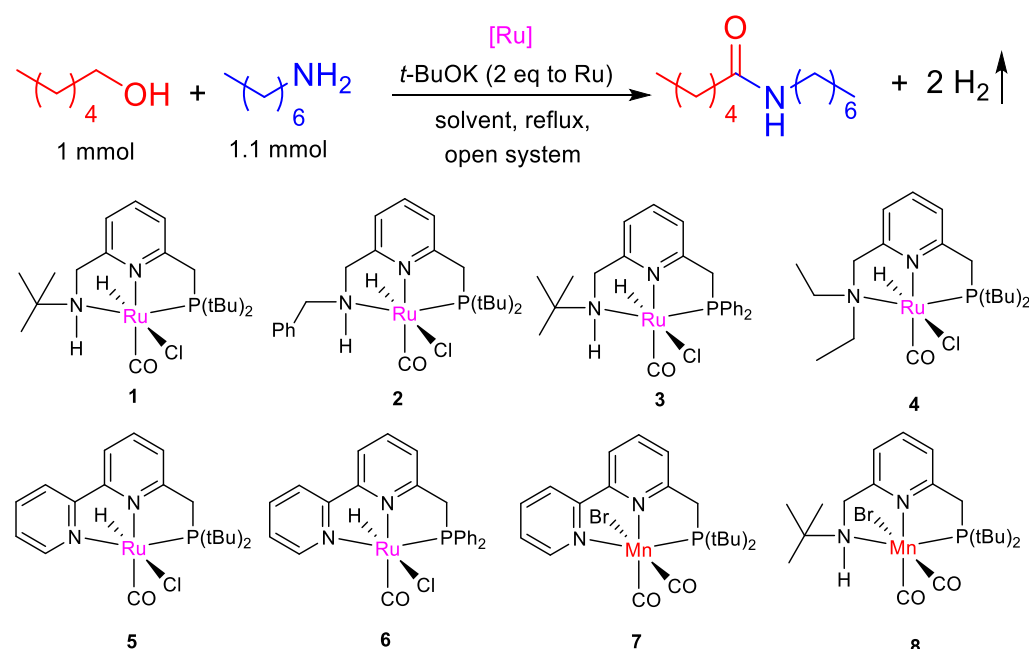


**Figure 1.** Selected examples of amide synthesis *via* dehydrogenative coupling of amines and alcohols.

**Table 1.** Conditions Screening for Low-Temperature Synthesis of *N*-Heptylhexanamide<sup>a</sup>



entry	[Ru]	solvent (b.p./°C)	time (h)	amide (%) <sup>b</sup>
1	1	Et <sub>2</sub> O (34.6)	12	11
2	2	Et <sub>2</sub> O	12	66
3	3	Et <sub>2</sub> O	12	0
4	4	Et <sub>2</sub> O	12	0
5	5	Et <sub>2</sub> O	12	1
6	6	Et <sub>2</sub> O	12	0
7	7	Et <sub>2</sub> O	12	0
8	8	Et <sub>2</sub> O	12	0
9 <sup>d</sup>	2	Et <sub>2</sub> O	22	92
10	2	MTBE (55.2)	12	97 (95) <sup>c</sup>

<sup>a</sup>Reaction conditions: 1-hexanol (1 mmol), 1-heptylamine (1.1 mmol), [Ru] (0.01 mmol), *t*-BuOK (0.02 mmol), solvent (2 mL), reflux with bath temperatures of 50 and 70 °C for Et<sub>2</sub>O and MTBE, respectively, time as specified. <sup>b</sup>Yields are calculated based on <sup>1</sup>H NMR spectra with mesitylene as an internal standard. <sup>c</sup>Isolated yield. <sup>d</sup>Reaction scaled down by a factor of 2 (solvent 2 mL).

dihydride intermediate. Wang and co-workers had computationally investigated the mechanism of this amide formation in detail with the traditional Ru–PNN<sub>Et</sub> Milstein complex, and according to their calculations, hydride abstraction from the alcohol and hemiaminal steps have activation barriers of around 25 and 31 kcal/mol, respectively.<sup>9</sup> The high energy requirement, especially for the hemiaminal dehydrogenation, is

in line with the elevated temperature required for the amide synthesis. Moreover, the overall formation of amide and H<sub>2</sub> from alcohol and amine is generally thermodynamically uphill, also contributing toward the high required temperature for amide synthesis. In this context, development of lower-temperature dehydrogenative amide synthesis protocols by rational catalyst design is desirable in order to improve the

Table 2. Dehydrogenative Synthesis of Various Amides at Low Temperature<sup>a</sup>

Entry	Alcohol	Amine	Amide	Solvent <sup>b</sup>	Time (h)	Yield (%) <sup>c</sup>
1				Et <sub>2</sub> O	22	92(85)
2				Et <sub>2</sub> O	22	97(92)
3				Et <sub>2</sub> O	24	91(82)
4				Et <sub>2</sub> O	22	88(83)
5				Et <sub>2</sub> O	40	87(81)
6				Et <sub>2</sub> O	36	89
7				Et <sub>2</sub> O	22	97(93)
8				Et <sub>2</sub> O	40	84
9 <sup>d</sup>				Et <sub>2</sub> O	40	73
10 <sup>d</sup>				Et <sub>2</sub> O	24	43
11				MTBE	24	84(71)
12 <sup>e</sup>				Et <sub>2</sub> O	36	40
13				MTBE	36	83(75)
14				MTBE	36	58
15				MTBE	22	5
16				Toluene	24	78(67)
17 <sup>f</sup>				MTBE	40	56
18 <sup>g</sup>				MTBE	20	(95)
19 <sup>h</sup>				MTBE	48	76(55)
20 <sup>i</sup>				MTBE	60	62(47)

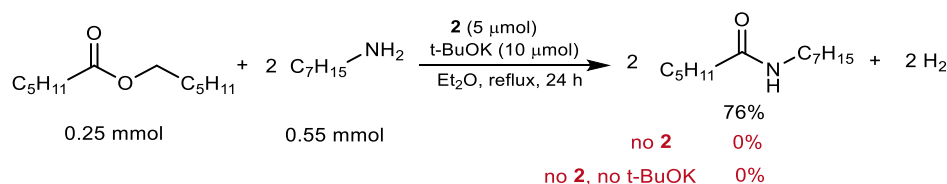
<sup>a</sup>Reaction conditions: alcohol (0.5 mmol), amine (0.55 mmol), **2** (0.005 mmol), *t*-BuOK (0.01 mmol), solvent (2 mL), reflux under Ar in an open system [the bath temperature was 50 °C (Et<sub>2</sub>O) or 70 °C (MTBE) or 130 °C (toluene)]. <sup>b</sup>b.p. under 1 atmospheric pressure. <sup>c</sup>Yields calculated similar to those in Table 1; in parentheses are isolated yields. <sup>d</sup>Rest of the alcohol unchanged. <sup>e</sup>Ester 10% observed, rest 50% of alcohol unchanged. <sup>f</sup>50 mol % KO<sup>t</sup>Bu. <sup>g</sup>Ethylenediamine (0.5 mmol), EtOH (1.5 mmol), **1** (0.005 mmol), and *t*-BuOK (0.01 mmol). <sup>h</sup>Cat (2 mol %), in a 100 mL closed flask. <sup>i</sup>Cat (2 mol %), in a 25 mL closed flask; the generated gas inside released intermittently after cooling down (24th and 48th h).

applicability of this atom-economical dehydrogenative coupling process.

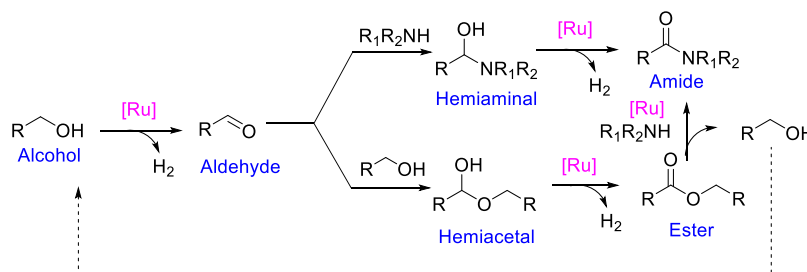
## RESULTS AND DISCUSSION

These considerations led us to explore the possibility of a low-temperature amide synthesis pathway *via* the acceptorless

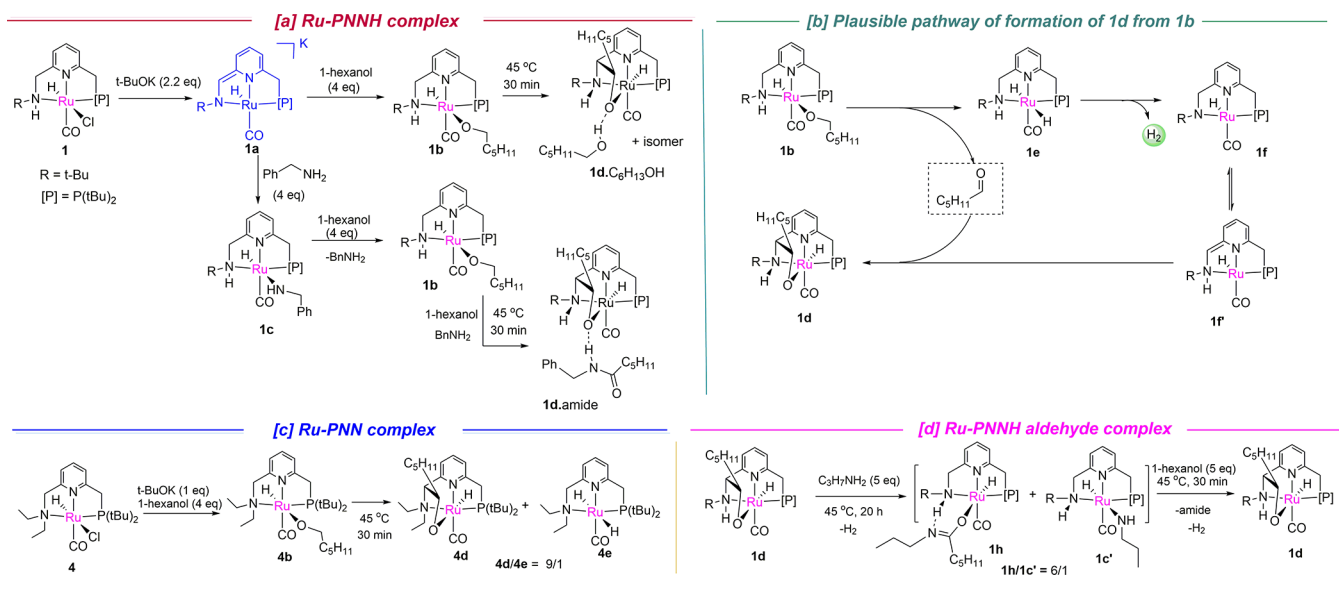
dehydrogenative coupling.<sup>10</sup> We started our investigation with the synthesis of *N*-heptylhexanamide by coupling of 1-hexanol and 1-heptylamine (Table 1). Several ruthenium and manganese pincer complexes were screened for the amide synthesis under Et<sub>2</sub>O reflux (boiling point 34.6 °C) in the presence of catalytic amounts of *t*-BuOK. Interestingly, among

Scheme 1. Amide Formation from Ester Catalyzed by **2**

Scheme 2. Pathway of Amide Formation



Scheme 3. Reactivity of Ru Complexes with the Base, Alcohol, and Amine



these complexes, Ru-PNNH complexes<sup>11</sup> **1** and **2**, featuring a terminal N–H moiety, displayed catalytic activities toward amide formation even at this low temperature (entries 1–2). Ru-PNNH complexes **1**–**3** are capable of two distinct modes of metal–ligand cooperation (MLC), amido–amine and aromatization–dearomatization,<sup>11</sup> unlike complexes **4**–**6**, where only aromatization–dearomatization is possible. Ru-P<sup>Ph</sup>NNH complex **3**, with electron-withdrawing Ph substituents on the P donor atom, did not show catalytic activity at this temperature (entry 3). Comparing **1** and **2**, the *N*-benzyl-substituted PNNH complex **2** showed higher activity than the *tert*-Bu-substituted complex **1**. The reason behind the higher activity of complex **2** is investigated in more detail during mechanistic investigations (*vide infra*).

Traditional PNN complexes, **4**–**6** (entries 4–6), with only one mode of MLC (aromatization–dearomatization) were not active at low temperature, although they can catalyze the reaction at the higher temperature of 110 °C (entries 4–8).<sup>5,6b</sup> Thus, the terminal N–H moiety of the Ru-PNNH complexes likely plays an important role in their low-temperature catalytic

activity. Mn-based PNN and PNNH complexes were also not active at this low temperature (entries 7–8). High conversion of 1-hexanol and 1-heptylamine to the corresponding amide was obtained with **2** as a pre-catalyst and diethyl ether as a solvent after 22 h of reflux (entry 9). A faster reaction was observed at a higher temperature such as reflux in the methyl *tert*-butyl ether (MTBE) solvent (b.p.: 55.2 °C) (entry 10). The generation of H<sub>2</sub> gas was confirmed by carrying out the reaction in a closed vessel and analyzing the headspace gas by gas chromatography after the reaction (Figure S5).

The substrate scope of this low-temperature amide synthesis system was subsequently explored (Table 2). Simple amides such as *N*-heptylhexanamide, *N*-benzylhexanamide, *N*-heptylbenzamide, *N*-benzylbenzamide, and *N*-(furfuryl)hexanamide were synthesized in high yields under refluxing conditions in diethyl ether (Table 2, entries 1–6). Besides primary amines, the secondary amine morpholine and 1-hexanol can also couple at low temperature in the presence of **2**, producing the tertiary amide *N*-hexanoylmorpholine in excellent yield (entry 7). Different halogen substituents such as –F and –Br are also

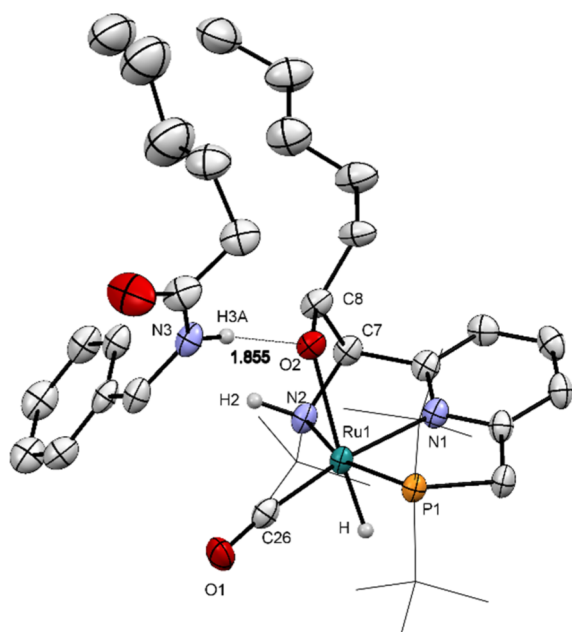


**Figure 2.** ORTEP diagram of complex **1d.amide**. Atoms are drawn with a probability level of 50%. Selected hydrogen atoms omitted for clarity. *Tert*-butyl groups displayed as a wireframe for clarity. Selected bond lengths (Å) and angles (°): Ru(1)–P(1) 2.2576(5), Ru(1)–O(2) 2.2380(15), Ru(1)–N(1) 2.0850(19), Ru(1)–N(2) 2.2010(17), Ru(1)–C(26) 1.818(2), O(2)–C(8) 1.394(3), C(7)–C(8) 1.570(3); P(1)–Ru(1)–H 81.5(11), O(2)–Ru(1)–P(1) 105.13(4), O(2)–Ru(1)–H 168.8(11), N(1)–Ru(1)–P(1) 81.81(5), N(1)–Ru(1)–O(2) 81.74(7), N(2)–Ru(1)–O(2) 72.92(6), C(8)–O(2)–Ru(1) 113.36(13), O(2)–C(8)–C(7) 109.38(18).

tolerated under the reaction conditions (entries 8–9). For the synthesis of some other amides, such as *N*-heptyl-2-methoxyacetamide and *N*-heptylisovaleramide, a slightly higher temperature was required for complete conversions (reflux in MTBE) (entries 10–13).<sup>5</sup> Highly reducible groups, such as a C–C double bond, are also tolerated under the conditions despite the reaction being associated with the evolution of H<sub>2</sub> gas (entry 14). It is to be noted that the nucleophilicity of the amine plays an important role in the rate of the reactions. For example, in the case of the synthesis of *N*-phenylhexanamide, the low nucleophilicity of aniline necessitates either a higher reaction temperature (reflux in toluene) or an increased base concentration (50 mol % KOtBu) for effective amidation (entries 15–17). Notably, ethylenediamine and ethanol can also dehydrogenatively couple at low temperatures (reflux in MTBE) in the presence of complex **2** to provide the diamide in 95% yield (entry 18). We also investigated the possibility of the synthesis of chiral amides *via* this method using a  $\beta$ -chiral alcohol and an  $\alpha$ -chiral amine. The chiral centers of the substrates were largely retained in the product amide molecules in both cases, as determined from optical rotation analysis of the products in comparison with literature data, demonstrating the potential utility of this method in the synthesis of biologically active amide molecules (entries 19–20, Figures S41 and S42).

In some of the reactions of Table 2 (entries 4, 5, 8, and 14), esters in moderate amounts were detected (~0–10%). To understand whether the generated ester is converted to the amide at this low temperature or is exclusively a competing reaction pathway, we set up a reaction of hexyl hexanoate with

1-heptylamine. After 24 h of refluxing in Et<sub>2</sub>O under similar reaction conditions, the formation of the corresponding amide, *N*-heptylhexanamide, in 76% yield was observed (Scheme 1), signifying that complex **2** can also catalyze the synthesis of amides from esters at low temperatures, presumably *via* initial nucleophilic substitution of the ester with the amine to form an amide and an alcohol, followed by dehydrogenative coupling between the released alcohol and amine to form amide.<sup>12</sup> In the absence of the ruthenium complex, no conversion of ester to amide was observed, signifying that the ruthenium complex catalyzes this reaction, likely acting as a Lewis acid to activate the ester during the initial amine nucleophilic attack on the ester.

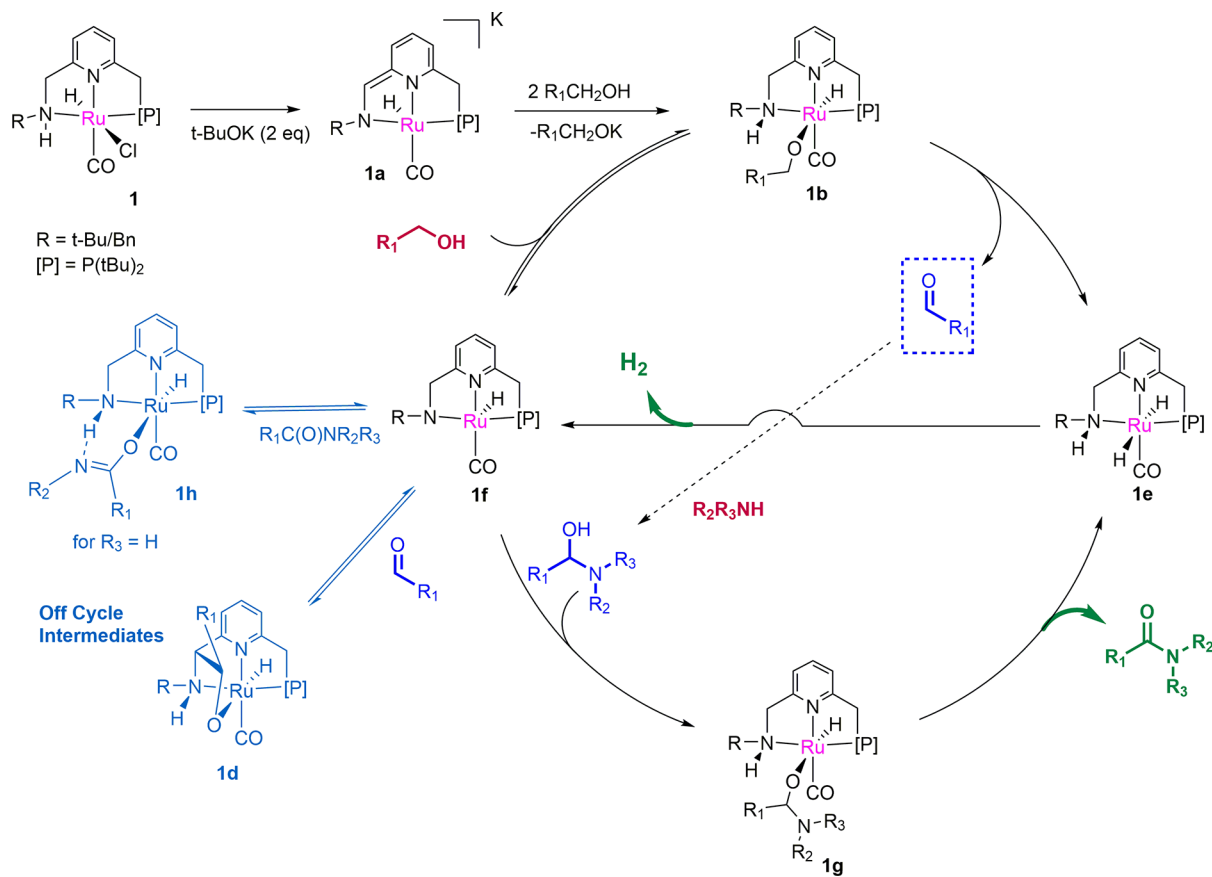
Based on these observations, the reaction pathway for the amide formation is shown in Scheme 2. The initial dehydrogenation of alcohol forms the aldehyde, which further converts to hemiaminal or hemiacetal *via* nucleophilic attack of the amine or alcohol, respectively. Subsequent dehydrogenation of the hemiaminal and hemiacetal intermediates produces the amide and ester, respectively. The ester is further converted to amide *via* nucleophilic substitution by the amine, assisted by the ruthenium complex under the reaction conditions.

Mechanistic studies were carried out to further understand the mechanism of the low-temperature catalytic activities of the PNNH complexes (Scheme 3). Complex **1**, upon addition of 2 eq of *t*-BuOK, forms the anionic complex **1a** which is intensely violet in diethyl ether solution (Scheme 3a).<sup>11</sup> Addition of 1-hexanol (4 equiv) to this complex results in the formation of the aromatic alkoxy complex **1b** (see Figure S20 for reaction progress). Noteworthy, the alkoxy ligand of **1b** exchanges quickly with the free alcohol in solution, and as the excess alcohol is removed from the solution, peak broadening in <sup>31</sup>P{<sup>1</sup>H} and <sup>1</sup>H NMR is observed.<sup>13</sup> Similar to the formation of the alkoxy complex, addition of benzylamine (4 equiv) to a solution of **1a** resulted in the formation of the amido complex **1c**. Further addition of alcohol to the amido complex replaced the amido ligand to form the alkoxy complex along with the generation of amine (Scheme 3a; Figure S21). On a similar note, addition of a 1/1 alcohol and amine solution to complex **1a** resulted in the selective formation of the alkoxy complex in solution.

When the resulting solution containing complex **1b**, amine, and alcohol was heated at 45 °C in a J. Young NMR tube, the formation of a new complex was observed after 30 min with almost quantitative conversion of **1b** (Scheme 3a; Figure S21). This complex exhibits a characteristic peak in the <sup>31</sup>P NMR at 119.4 ppm (major isomer) (Figure S14).<sup>14</sup> In the proton NMR, a hydride peak corresponding to this complex was observed at –15.2 ppm as a doublet (*J* = 28.5 Hz) (Figure S8). In the IR spectrum, a strong absorption band at 1900 cm<sup>–1</sup> was observed, corresponding to a CO ligand. Interestingly, the <sup>13</sup>C NMR spectrum indicated the activation of the *N*-arm as the secondary picolylic CH<sub>2</sub> unit of the *N*-arm was converted to a tertiary CH unit along with another CH unit, presumably from an alcohol derivative (Figure S11). Based on 1D and 2D NMR analysis, the structure of **1d** was assigned to a new complex where an *in situ* generated aldehyde binds to the *N*-arm of the ligand through MLC. Single crystals suitable for X-ray diffraction (XRD) analysis were grown by slow evaporation from a THF/pentane solution of **1d**, and the XRD analysis confirmed the assigned structure of **1d** (Scheme 3a, Figure 2). Interestingly, in the unit cell of the crystal, a product amide



Scheme 4. Plausible Mechanistic Cycle



molecule of *N*-benzylhexanamide was found attached to **1d**, forming **1d**.amide *via* hydrogen bonding (Figure 2). The aldehyde addition across the metal and ligand arm has been documented before by us with a Ru–PNP system at much lower temperatures ( $-78\text{ }^{\circ}\text{C}$ )<sup>13</sup> and also by Sanford and co-workers with the traditional Ru–PNNet<sub>2</sub> system at room temperature following the addition of benzaldehyde to the dearomatized complexes.<sup>15</sup> However, it is quite interesting that this aldehyde complex can also be readily and quantitatively accessed from the alkoxy complex upon brief, mild heating, signifying the possible generation of dearomatized complexes during the reaction.

Complex **1d** can also be accessed upon heating the alkoxy complex **1b** in the presence of alcohol but without amine, forming an alcohol adduct **1d**.C<sub>6</sub>H<sub>13</sub>OH (Scheme 3a), as verified by NMR analysis (Figures S8 and S9). The formation of **1d** from **1b** presumably happens *via* the formation of the dihydride **1e**, followed by the formation of amido complex **1f** with the evolution of H<sub>2</sub> (Scheme 3b). The amido complex **1f** can further convert to the *N*-arm dearomatized complex **1f'**, to which the addition of aldehyde affords complex **1d** (Scheme 3b). However, the dihydride complex was not observed by NMR, signifying that the H<sub>2</sub> elimination from the dihydride complex **1e** is facile. A similar aldehyde adduct complex also forms with the traditional Ru–PNNet<sub>2</sub> complex **4** at  $45\text{ }^{\circ}\text{C}$  in the presence of a base and alcohol, although, in this case, the dihydride complex is also observed in the NMR (Scheme 3c, Figure S22). This signifies that (i) even in the case of Ru–PNNet<sub>2</sub>, the first alcohol dehydrogenation step can proceed at low temperature, at least, stoichiometrically, and (ii) H<sub>2</sub>

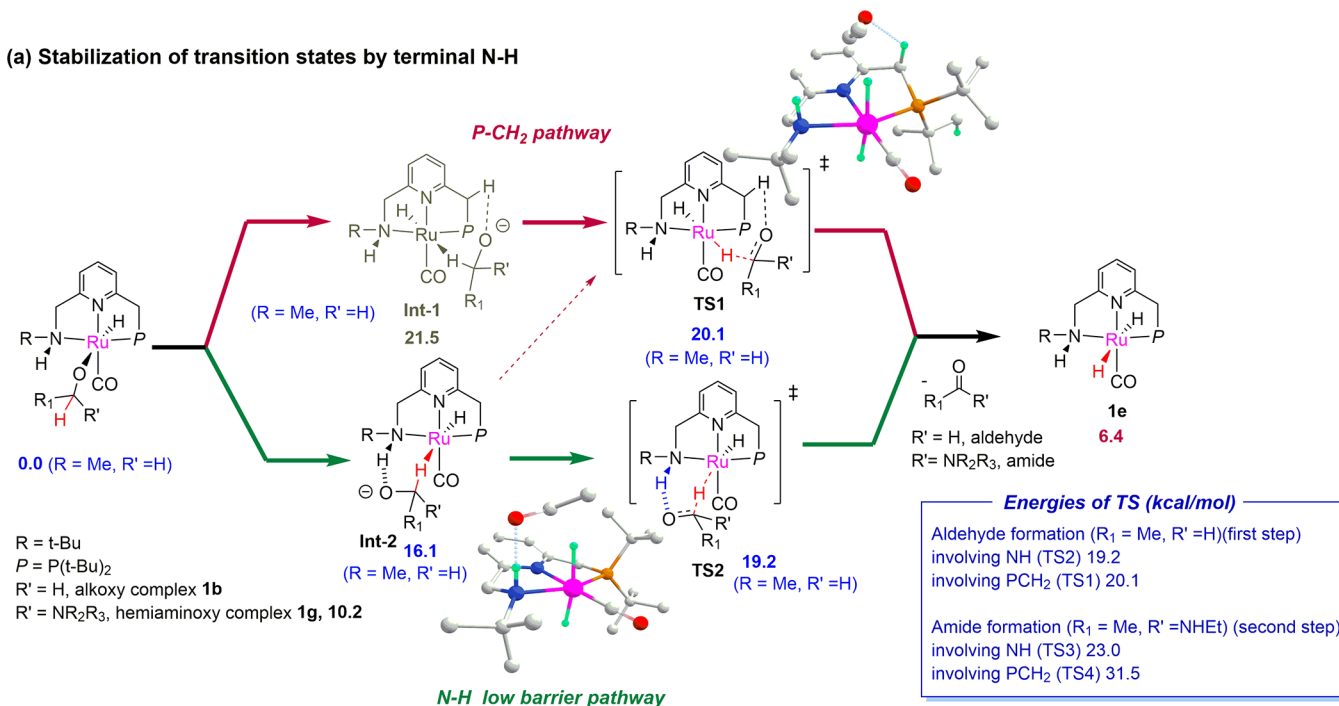
generation from **1e** is more facile than from the dihydride complex **4e**, presumably due to the new mode of MLC *via* the involvement of the terminal N–H moiety.

The aldehyde binding to the side arm in complex **1d** is reversible and rapidly exchanges with free benzaldehyde in solution as verified by an aldehyde-exchange experiment (Figure S23).<sup>16</sup> Complex **1d**, upon addition of *n*-propylamine (5 equiv), followed by mild heating ( $45\text{ }^{\circ}\text{C}$ ), gradually formed a new complex (Scheme 3d) in which the C–C bond was broken as concluded from <sup>1</sup>H and <sup>31</sup>P{<sup>1</sup>H} NMR. The transformation is also associated with the formation of H<sub>2</sub> gas, as expected. Based on the NMR analysis, the new complex is assigned the structure of the amidate complex **1h**, which is formed *via* addition of the *in situ* generated amide product to the amido complex **1f** (Scheme 4). We have previously observed the reversible formation of similar amidate complexes upon addition of amide to the dearomatized PNNH complexes.<sup>17</sup> The formation of complex **1c'** was also observed in a minor amount resulting from the addition of free amine to complex **1f** (Scheme 3d, Figure S26). The amidate and amido ligands from **1h** and **1c'** are gradually replaced in the presence of 1-hexanol (5 equiv) at  $45\text{ }^{\circ}\text{C}$ , regenerating complex **1d** (Scheme 3d, Figure S26). These results clearly demonstrate the competing binding routes of different substrates, intermediates, and products to the PNNH amido complex that are operational during active catalysis (Scheme S1).

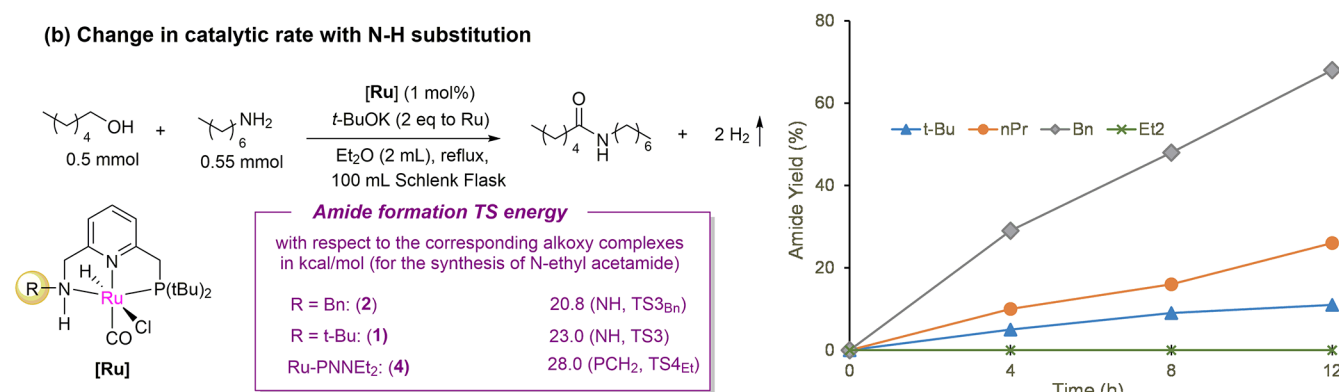
Based on the mechanistic experiments and on prior investigation by our group and others on the dehydrogenative amide bond formation, we propose a catalytic cycle as depicted in Scheme 4. The pre-catalyst, in the presence of the base and

Scheme 5. Importance of the Terminal N–H Moiety<sup>a</sup>

## (a) Stabilization of transition states by terminal N–H



## (b) Change in catalytic rate with N–H substitution

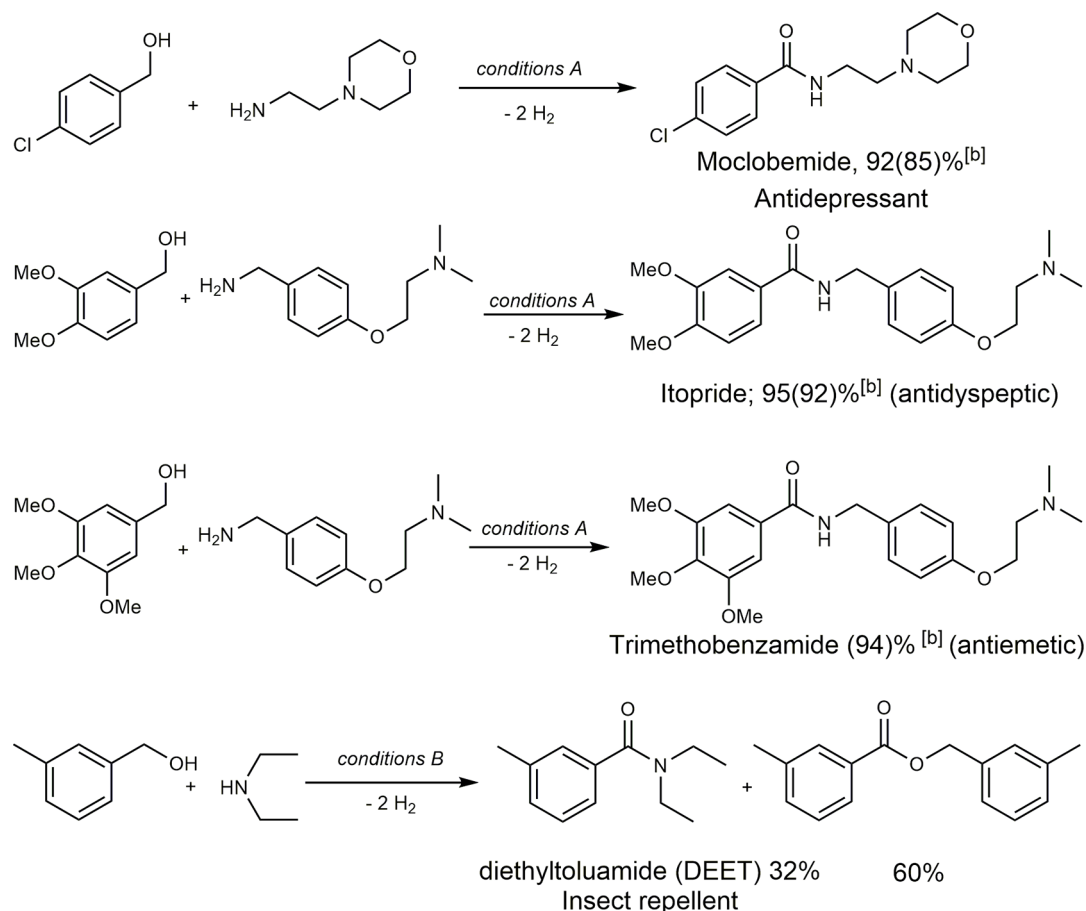


<sup>a</sup>Energy values correspond to Gibbs free energies (kcal mol<sup>−1</sup>) with respect to the ethoxy complex + ethylamine at 298.15 K in a diethyl ether continuum. All reactant concentrations are 1 M, except for H<sub>2</sub> which is at 1 atm. Mass balance is ensured throughout.

alcohol, forms the alkoxy complex **1b**. Hydride elimination from the alkoxy ligand through an outer-sphere mechanism (Scheme 5a, *vide infra*) forms the dihydride complex **1e**, along with the aldehyde. Subsequently, H<sub>2</sub> elimination from the dihydride forms the amido complex **1f**. This H<sub>2</sub> evolution from the dihydride complex can happen by itself or through the assistance of an alcohol molecule. The amido complex then binds to the aldehyde to form the likely off-cycle intermediate complex **1d** (via a pathway as depicted in Scheme 3b) which is also the catalytic resting state of the reaction. **1d**, in the presence of an amine, generates the hemiaminoxy complex **1g**, presumably via the formation of **1f**. In the subsequent reaction step, hydride elimination from the hemiaminoxy complex generates the amide and the dihydride complex again. Further H<sub>2</sub> elimination from the dihydride complex **1e**, followed by the addition of alcohol to the resulting amido complex, regenerates the alkoxy complex **1b**, closing the catalytic cycle. It is to be noted that based on our experimental evidence, we cannot

exclude the possibility of a beta hydride elimination pathway via N-arm opening, although this route is calculated to have higher energy requirement than the stepwise outer-sphere pathway for the traditional Ru–PNNEt<sub>2</sub> complex.<sup>9</sup>

The hydride abstraction from the alkoxy and the hemiaminoxy complexes, leading to the formation of the aldehyde and amide, respectively, and the dihydride complex, is proposed to proceed via the formation of a high-energy intermediate where the hydrogen atom coordinates to the metal center (Scheme 5a, Int 1–2).<sup>9,18</sup> This step is also associated with a high activation barrier, especially the amide formation step, which has been previously computed to be the highest energy-requiring step in the case of the PNNEt<sub>2</sub> system.<sup>9</sup> In the case of the PNNEt<sub>2</sub> system, this hydride abstraction transition state can proceed via the involvement of the picolyl CH<sub>2</sub> protons. Our computation suggests that in the case of the PNNH system, the terminal N–H moiety can allow the mechanism to proceed via a low-energy pathway. For

Scheme 6. Synthesis of Various Pharmaceutical Drugs<sup>a</sup>

<sup>a</sup>Conditions A: alcohol (0.5 mmol), amine (0.6 mmol), **2** (0.005 mmol), *t*-BuOK (0.01 mmol), MTBE (2 mL, bp 55.2 °C), reflux (bath temp. 70 °C), 60 h. Conditions B: alcohol (0.5 mmol), amine (5 mmol), **1** (0.005 mmol), *t*-BuOK (0.01 mmol), K<sub>3</sub>PO<sub>4</sub> (0.5 mmol), dioxane (2 mL), reflux in a closed tube for 60 h (see the [Supporting Information](#) for details). <sup>b</sup>Yields in parentheses are isolated yields, and yields outside parentheses are <sup>1</sup>H NMR yields.

example, the pathway involving the terminal N–H is 0.9 kcal/mol lower in energy for the aldehyde formation step than the PCH<sub>2</sub> pathway. On the other hand, for the amide formation step, which is also a higher energy-demanding step compared to the aldehyde formation, the new pathway was found to be 8.5 kcal/mol lower in energy (Scheme 5a). This additional stabilization likely explains the high catalytic activities of the PNNH complexes at low reaction temperatures. Please note that although we compute here a stepwise outer-sphere reaction pathway, the possibility of a concerted outer-sphere reaction pathway involving simultaneous proton and hydride transfer from the substrate to the ligand and metal, respectively, similar to the mechanisms associated with many reactions with Noyori and Shvo's catalysts, cannot be ruled out (Scheme S2).<sup>19</sup> Nevertheless, the concerted mechanism can also be surmised to be more stabilized by the terminal N–H route as compared to the P–CH<sub>2</sub> one.

Further support of the importance of the N–H proton and its acidity is obtained from comparing the catalysis rate of different Ru–PNNH complexes. As is seen in Table 1 and Scheme 5b, a significant increase in the catalytic activity was observed when the N substitution of the Ru–PNNH complex was changed from *tert*-butyl to the benzyl group. To understand whether this change in activity is likely due to steric or electronic factors, we synthesized the novel *N*-propyl

derivative of Ru–PNNH complex **9** (synthesis methods and characterization data are in the [Supporting Information](#)). The catalytic activity of the *n*-Pr Ru–PNNH analogue was found to be in between those of the *t*-Bu and Bn analogues under similar reaction conditions (Scheme 5b). This suggests that the higher activity of the benzyl derivative likely results from the electronic properties of the benzyl group since *n*-Pr and the benzyl moiety display similar steric bulks around the N donor. In the case of the benzyl substitution, the terminal N–H is more acidic, likely providing the highest stabilization to the transition state of hydride elimination from alkoxy and hemiaminoxy complexes. In addition, based on the density functional theory calculations, an overall lower activation energy was computed for the amide formation in the PNNH<sub>Bn</sub> system compared to the PNNH<sub>*t*Bu</sub> system and the PNNH<sub>*n*Pr</sub> system (Scheme 5b). Thus, the acidity of the N–H bond is an important factor influencing the low-temperature catalytic activity of these complexes. This also hints at a possible avenue toward developing more efficient catalysts, perhaps functioning under even ambient conditions.

We also synthesized several commercially available amide bond-containing pharmaceuticals *via* this method at low temperatures to demonstrate its utility (Scheme 6). Despite the activity of several complexes toward catalyzing the dehydrogenative formation of the amide bond, the synthesis



of even simple pharmaceutical drugs *via* this atom-economical method has not been demonstrated until now, even at higher reaction temperatures.<sup>20</sup> Moclobemide is a reversible inhibitor of monoamine oxidase A, approved as an antidepressant in United Kingdom and Canada.<sup>21</sup> Using the dehydrogenative coupling method, moclobemide was conveniently synthesized from the corresponding alcohol and amine in 92% yield (isolated yield 85%) upon refluxing in MTBE with **1** as a catalyst.<sup>22</sup> Notably, with H<sub>2</sub> being the only byproduct of the reaction, the resulting moclobemide can be easily purified by recrystallization in the cold diethyl ether/pentane solvent mixture without the requirement of purification by column chromatography. Similarly, the antidyspeptic drug itopride (brand name: Ganaton)<sup>23</sup> and the antiemetic trimethobenzamide were synthesized from the corresponding alcohol and amine with 92 and 94% yields, respectively, under similar reaction conditions, without the requirement of purification *via* column chromatography. In the case of the insect repellent diethyltoluamide, it was synthesized in 32% yield *via* this method at higher temperatures (reflux in 1,4-dioxane) and in the presence of 1 eq K<sub>3</sub>PO<sub>4</sub> due to lower nucleophilicity of the secondary amine compared to the primary ones.<sup>6b</sup> Further investigation on the synthesis of more complex pharmaceuticals *via* this method through catalyst improvement and condition optimization is ongoing in our group.

## CONCLUSIONS

In summary, we report the near-ambient-temperature dehydrogenative formation of the amide bond (reflux in Et<sub>2</sub>O) from alcohols and amines. The Ru–PNNH complexes, featuring a terminal N–H unit, showed remarkable catalytic activities at this low temperature. This high activity is presumably due to the new catalytic pathway involving the terminal N–H moiety, and the acidity of this terminal N–H heavily influenced the low-temperature catalytic rate. An unusual resting state of the complex during catalysis was observed, where the aldehyde binds between the N-side arm and Ru center of the complex *via* a reversible C–C bond formation. Using Ru–PNNH complex **2**, we synthesized several amides under refluxing conditions in Et<sub>2</sub>O or MTBE. Furthermore, several amide bonds containing commercially available pharmaceuticals, including moclobemide, itopride, and trimethobenzamide, were prepared at low temperature *via* this atom-economical method. Our future efforts in this context will be aimed toward the development of even more efficient catalysts for this transformation based on the mechanistic insights gained during this study as well as toward the synthesis of more complex pharmaceuticals *via* this method.

## ASSOCIATED CONTENT

### Supporting Information

The Supporting Information is available free of charge at <https://pubs.acs.org/doi/10.1021/acscatal.1c00728>.

General information and experimental details (PDF)

Crystallographic data of compounds (CIF)

## AUTHOR INFORMATION

### Corresponding Author

David Milstein – Department of Molecular Chemistry and Materials Science, The Weizmann Institute of Science, Rehovot 76100, Israel; [orcid.org/0000-0002-2320-0262](https://orcid.org/0000-0002-2320-0262); Email: [david.milstein@weizmann.ac.il](mailto:david.milstein@weizmann.ac.il)

## Authors

Sayan Kar – Department of Molecular Chemistry and Materials Science, The Weizmann Institute of Science, Rehovot 76100, Israel; [orcid.org/0000-0002-6986-5796](https://orcid.org/0000-0002-6986-5796)

Yinjun Xie – Department of Molecular Chemistry and Materials Science, The Weizmann Institute of Science, Rehovot 76100, Israel; Present Address: Ningbo Institute of Materials Technology & Engineering, Chinese Academy of Sciences, Ningbo, 315201, P.R. China

Quan Quan Zhou – Department of Molecular Chemistry and Materials Science, The Weizmann Institute of Science, Rehovot 76100, Israel

Yael Diskin-Posner – Department of Chemical Research Support, The Weizmann Institute of Science, Rehovot 76100, Israel; [orcid.org/0000-0002-9008-8477](https://orcid.org/0000-0002-9008-8477)

Yehoshua Ben-David – Department of Molecular Chemistry and Materials Science, The Weizmann Institute of Science, Rehovot 76100, Israel

Complete contact information is available at:

<https://pubs.acs.org/doi/10.1021/acscatal.1c00728>

## Author Contributions

<sup>§</sup>S.K. and Y.X. contributed equally.

## Notes

The authors declare no competing financial interest.

Synthetic procedures, NMR spectra, and characterization data for all the new compounds are available within this article and its Supporting Information. The X-ray crystallographic coordinates for the structure reported in this article have been deposited at the Cambridge Crystallographic Data Centre (CCDC) under deposition number CCDC 2043153. The data can be obtained free of charge from The Cambridge Crystallographic Data Centre *via* [http://www.ccdc.cam.ac.uk/data\\_request/cif](http://www.ccdc.cam.ac.uk/data_request/cif). Any further relevant data are available from the authors upon reasonable request.

## ACKNOWLEDGMENTS

Dedicated to Prof. Christian Bruneau for his outstanding contribution to catalysis. This research was supported by the European Research Council (ERC AdG 692775). D.M. holds the Israel Matz Professorial Chair of Organic Chemistry. S.K. acknowledges the Sustainability and Energy Research Initiative (SAERI) of the Weizmann Institute of Science for a research fellowship.

## REFERENCES

- (1) (a) Cupido, T.; Tulla-Puche, J.; Spengler, J.; Albericio, F. The synthesis of naturally occurring peptides and their analogs. *Curr. Opin. Drug Discovery Dev.* **2007**, *10*, 768–783. (b) Hu, P.; Ben-David, Y.; Milstein, D. Rechargeable Hydrogen Storage System Based on the Dehydrogenative Coupling of Ethylenediamine with Ethanol. *Angew. Chem., Int. Ed.* **2016**, *55*, 1061–1064. (c) Hu, P.; Fogler, E.; Diskin-Posner, Y.; Iron, M. A.; Milstein, D. A novel liquid organic hydrogen carrier system based on catalytic peptide formation and hydrogenation. *Nat. Commun.* **2015**, *6*, 6859. (d) Xie, Y.; Hu, P.; Ben-David, Y.; Milstein, D. A Reversible Liquid Organic Hydrogen Carrier System Based on Methanol-Ethylenediamine and Ethylene Urea. *Angew. Chem., Int. Ed.* **2019**, *58*, 5105–5109.
- (2) (a) Carey, J. S.; Laffan, D.; Thomson, C.; Williams, M. T. Analysis of the reactions used for the preparation of drug candidate molecules. *Org. Biomol. Chem.* **2006**, *4*, 2337–2347. (b) Dunetz, J. R.; Magano, J.; Weisenburger, G. A. Large-Scale Applications of Amide Coupling Reagents for the Synthesis of Pharmaceuticals. *Org. Process Res. Dev.* **2016**, *20*, 140–177.

- (3) (a) Han, S.-Y.; Kim, Y.-A. Recent development of peptide coupling reagents in organic synthesis. *Tetrahedron* **2004**, *60*, 2447–2467. (b) Valeur, E.; Bradley, M. Amide bond formation: beyond the myth of coupling reagents. *Chem. Soc. Rev.* **2009**, *38*, 606–631. (c) de Figueiredo, R. M.; Suppo, J.-S.; Campagne, J.-M. Nonclassical Routes for Amide Bond Formation. *Chem. Rev.* **2016**, *116*, 12029–12122. (d) Montalbetti, C. A. G. N.; Falque, V. Amide bond formation and peptide coupling. *Tetrahedron* **2005**, *61*, 10827–10852. (e) Sabatini, M. T.; Boulton, L. T.; Sneddon, H. F.; Sheppard, T. D. A green chemistry perspective on catalytic amide bond formation. *Nat. Catal.* **2019**, *2*, 10–17.
- (4) (a) Constable, D. J. C.; Dunn, P. J.; Hayler, J. D.; Humphrey, G. R.; Leazer, J. L.; Linderman, R. J.; Lorenz, K.; Manley, J.; Pearlman, B. A.; Wells, A.; Zaks, A.; Zhang, T. Y. Key green chemistry research areas—a perspective from pharmaceutical manufacturers. *Green Chem.* **2007**, *9*, 411–420. (b) Bandichhor, R.; Bhattacharya, A.; Diorazio, L.; Dunn, P.; Fraunhofer, K.; Gallou, F.; Hayler, J.; Hickey, M.; Hinkley, B.; Hughes, D.; Humphreys, L.; Kaptein, B.; Mathew, S.; Oh, L.; Richardson, P.; White, T.; Wuyts, S. Green Chemistry Articles of Interest to the Pharmaceutical Industry. *Org. Process Res. Dev.* **2013**, *17*, 1394–1405.
- (5) Gunanathan, C.; Ben-David, Y.; Milstein, D. Direct Synthesis of Amides from Alcohols and Amines with Liberation of H<sub>2</sub>. *Science* **2007**, *317*, 790.
- (6) (a) Lane, E. M.; Uttley, K. B.; Hazari, N.; Bernskoetter, W. Iron-Catalyzed Amide Formation from the Dehydrogenative Coupling of Alcohols and Secondary Amines. *Organometallics* **2017**, *36*, 2020–2025. (b) Srimani, D.; Balaraman, E.; Hu, P.; Ben-David, Y.; Milstein, D. Formation of Tertiary Amides and Dihydrogen by Dehydrogenative Coupling of Primary Alcohols with Secondary Amines Catalyzed by Ruthenium Bipyridine-Based Pincer Complexes. *Adv. Synth. Catal.* **2013**, *355*, 2525–2530. (c) Gusev, D. G. Rethinking the Dehydrogenative Amide Synthesis. *ACS Catal.* **2017**, *7*, 6656–6662. (d) Chen, C.; Verpoort, F.; Wu, Q. Atom-economic dehydrogenative amide synthesis via ruthenium catalysis. *RSC Adv.* **2016**, *6*, 55599–55607. (e) Crochet, P.; Cadierno, V. Ruthenium-Catalyzed Amide-Bond Formation. In *Ruthenium in Catalysis*; Dixneuf, P. H., Bruneau, C., Eds.; Springer International Publishing: Cham, 2014; pp 81–118. (f) Schley, N. D.; Dobereiner, G. E.; Crabtree, R. H. Oxidative Synthesis of Amides and Pyrroles via Dehydrogenative Alcohol Oxidation by Ruthenium Diphosphine Diamine Complexes. *Organometallics* **2011**, *30*, 4174–4179. (g) Nordström, L. U.; Vogt, H.; Madsen, R. Amide Synthesis from Alcohols and Amines by the Extrusion of Dihydrogen. *J. Am. Chem. Soc.* **2008**, *130*, 17672–17673. (h) Zweifel, T.; Naubron, J.-V.; Grützmacher, H. Catalyzed Dehydrogenative Coupling of Primary Alcohols with Water, Methanol, or Amines. *Angew. Chem., Int. Ed.* **2009**, *48*, 559–563. (i) Ghosh, S. C.; Muthaiah, S.; Zhang, Y.; Xu, X.; Hong, S. H. Direct Amide Synthesis from Alcohols and Amines by Phosphine-Free Ruthenium Catalyst Systems. *Adv. Synth. Catal.* **2009**, *351*, 2643–2649. (j) Muthaiah, S.; Ghosh, S. C.; Jee, J.-E.; Chen, C.; Zhang, J.; Hong, S. H. Direct Amide Synthesis from Either Alcohols or Aldehydes with Amines: Activity of Ru(II) Hydride and Ru(0) Complexes. *J. Org. Chem.* **2010**, *75*, 3002–3006. (k) Prades, A.; Peris, E.; Albrecht, M. Oxidations and Oxidative Couplings Catalyzed by Triazolylidene Ruthenium Complexes. *Organometallics* **2011**, *30*, 1162–1167. (l) Spasyuk, D.; Vicent, C.; Gusev, D. G. Chemoselective Hydrogenation of Carbonyl Compounds and Acceptorless Dehydrogenative Coupling of Alcohols. *J. Am. Chem. Soc.* **2015**, *137*, 3743–3746. (m) Mondal, A.; Subramanian, M.; Nandakumar, A.; Balaraman, E. Manganese-Catalyzed Direct Conversion of Ester to Amide with Liberation of H<sub>2</sub>. *Org. Lett.* **2018**, *20*, 3381–3384. (n) Kothandaraman, J.; Kar, S.; Sen, R.; Goepfert, A.; Olah, G. A.; Prakash, G. K. S. Efficient Reversible Hydrogen Carrier System Based on Amine Reforming of Methanol. *J. Am. Chem. Soc.* **2017**, *139*, 2549–2552. (o) Fu, Z.; Lee, J.; Kang, B.; Hong, S. H. Dehydrogenative Amide Synthesis: Azide as a Nitrogen Source. *Org. Lett.* **2012**, *14*, 6028–6031. (p) Selvamurugan, S.; Ramachandran, R.; Prakash, G.; Nirmala, M.; Viswanathamurthi, P.; Fujiwara, S.; Endo, A. Ruthenium(II) complexes encompassing 2-oxo-1,2-dihydroquinoline-3-carbaldehyde thiosemicarbazone hybrid ligand: A new versatile potential catalyst for dehydrogenative amide synthesis. *Inorg. Chim. Acta* **2017**, *454*, 46–53. (q) Li, L.; Lei, M.; Liu, L.; Xie, Y.; Schaefer, H. F. Metal–Substrate Cooperation Mechanism for Dehydrogenative Amidation Catalyzed by a PNN-Ru Catalyst. *Inorg. Chem.* **2018**, *57*, 8778–8787. (r) Saha, B.; Sengupta, G.; Sarbajna, A.; Dutta, I.; Bera, J. K. Amide synthesis from alcohols and amines catalyzed by a RuII–N-heterocyclic carbene (NHC)–carbonyl complex. *J. Organomet. Chem.* **2014**, *771*, 124–130. (s) Cho, D.; Ko, K. C.; Lee, J. Y. Catalytic Mechanism for the Ruthenium-Complex-Catalyzed Synthesis of Amides from Alcohols and Amines: A DFT Study. *Organometallics* **2013**, *32*, 4571–4576. (t) Choi, G.; Hong, S. H. Selective N-Formylation and N-Methylation of Amines Using Methanol as a Sustainable C1 Source. *ACS Sustainable Chem. Eng.* **2019**, *7*, 716–723.
- (7) Kumar, A.; Espinosa-Jalapa, N. A.; Leitun, G.; Diskin-Posner, Y.; Avram, L.; Milstein, D. Direct Synthesis of Amides by Dehydrogenative Coupling of Amines with either Alcohols or Esters: Manganese Pincer Complex as Catalyst. *Angew. Chem., Int. Ed.* **2017**, *56*, 14992–14996.
- (8) (a) Shimizu, K.-i.; Ohshima, K.; Satsuma, A. Direct Dehydrogenative Amide Synthesis from Alcohols and Amines Catalyzed by  $\gamma$ -Alumina Supported Silver Cluster. *Chem.—Eur. J.* **2009**, *15*, 9977–9980. (b) Zhu, J.; Zhang, Y.; Shi, F.; Deng, Y. Dehydrogenative amide synthesis from alcohol and amine catalyzed by hydroxycitric acid-supported gold nanoparticles. *Tetrahedron Lett.* **2012**, *53*, 3178–3180. (c) Hakim Siddiki, S. M. A.; Toyao, T.; Shimizu, K.-i. Acceptorless dehydrogenative coupling reactions with alcohols over heterogeneous catalysts. *Green Chem.* **2018**, *20*, 2933–2952.
- (9) Li, H.; Wang, X.; Huang, F.; Lu, G.; Jiang, J.; Wang, Z.-X. Computational Study on the Catalytic Role of Pincer Ruthenium(II)-PNN Complex in Directly Synthesizing Amide from Alcohol and Amine: The Origin of Selectivity of Amide over Ester and Imine. *Organometallics* **2011**, *30*, 5233–5247.
- (10) Gunanathan, C.; Milstein, D. Applications of Acceptorless Dehydrogenation and Related Transformations in Chemical Synthesis. *Science* **2013**, *341*, 1229712.
- (11) (a) Fogler, E.; Garg, J. A.; Hu, P.; Leitun, G.; Shimon, L. J. W.; Milstein, D. System with Potential Dual Modes of Metal–Ligand Cooperation: Highly Catalytically Active Pyridine-Based PNNH–Ru Pincer Complexes. *Chem.—Eur. J.* **2014**, *20*, 15727–15731. He, T.; Buttner, J. C.; Reynolds, E. F.; Pham, J.; Malek, J. C.; Keith, J. M.; Chianese, A. R. Dehydroalkylative Activation of CNN- and PNN-Pincer Ruthenium Catalysts for Ester Hydrogenation. *J. Am. Chem. Soc.* **2019**, *141*, 17404–17413. (c) Pham, J.; Jarczyk, C. E.; Reynolds, E. F.; Kelly, S. E.; Kim, T.; He, T.; Keith, J. M.; Chianese, A. R. The key role of the latent N–H group in Milstein's catalyst for ester hydrogenation. *Chem. Sci.* **2021**, DOI: 10.1039/D1SC00703C.
- (12) Gnanaprakasam, B.; Milstein, D. Synthesis of Amides from Esters and Amines with Liberation of H<sub>2</sub> under Neutral Conditions. *J. Am. Chem. Soc.* **2011**, *133*, 1682–1685.
- (13) Montag, M.; Zhang, J.; Milstein, D. Aldehyde Binding through Reversible C–C Coupling with the Pincer Ligand upon Alcohol Dehydrogenation by a PNP–Ruthenium Catalyst. *J. Am. Chem. Soc.* **2012**, *134*, 10325–10328.
- (14) A minor isomer of complex **1d** was also observed (9%) in the solution, with a chemical shift of 121 ppm in the <sup>31</sup>P NMR spectrum and a hydride chemical shift of –15.1 ppm in the <sup>1</sup>H NMR spectrum.
- (15) Huff, C. A.; Kampf, J. W.; Sanford, M. S. Reversible carbon–carbon bond formation between carbonyl compounds and a ruthenium pincer complex. *Chem. Commun.* **2013**, *49*, 7147–7149.
- (16) Similarly the benzaldehyde bound complex (**1d'**) also exchanges the bound benzaldehyde with free hexanal/*p*-Cl benzaldehyde when excess hexanal (10 equiv) or *p*-Cl benzaldehyde is added to a solution of **1d** (Figures S24 and 25).
- (17) Kar, S.; Rauch, M.; Kumar, A.; Leitun, G.; Ben-David, Y.; Milstein, D. Selective Room-Temperature Hydrogenation of Amides

to Amines and Alcohols Catalyzed by a Ruthenium Pincer Complex and Mechanistic Insight. *ACS Catal.* **2020**, *10*, 5511–5515.

(18) (a) Alberico, E.; Lennox, A. J. J.; Vogt, L. K.; Jiao, H.; Baumann, W.; Drexler, H.-J.; Nielsen, M.; Spannenberg, A.; Checinski, M. P.; Junge, H.; Beller, M. Unravelling the Mechanism of Basic Aqueous Methanol Dehydrogenation Catalyzed by Ru–PNP Pincer Complexes. *J. Am. Chem. Soc.* **2016**, *138*, 14890–14904. (b) Zou, Y. Q.; Wolff, N.; Rauch, M.; Feller, M.; Zhou, Q. Q.; Anaby, A.; Diskin-Posner, Y.; Shimon, L. J. W.; Avram, L.; Ben-David, Y.; Milstein, D. Homogeneous Reforming of Aqueous Ethylene Glycol to Glycolic Acid and Pure Hydrogen Catalyzed by Pincer-Ruthenium Complexes Capable of Metal–Ligand Cooperation. *Chem.—Eur. J.* **2021**, *27*, 4715–4722. (c) Gusev, D. G. Revised Mechanisms of the Catalytic Alcohol Dehydrogenation and Ester Reduction with the Milstein PNN Complex of Ruthenium. *Organometallics* **2020**, *39*, 258–270.

(19) (a) Dub, P. A.; Gordon, J. C. The role of the metal-bound N–H functionality in Noyori-type molecular catalysts. *Nat. Rev. Chem.* **2018**, *2*, 396–408. (b) Samec, J. S. M.; Bäckvall, J.-E.; Andersson, P. G.; Brandt, P. Mechanistic aspects of transition metal-catalyzed hydrogen transfer reactions. *Chem. Soc. Rev.* **2006**, *35*, 237–248. (c) Johnson, J. B.; Bäckvall, J.-E. Mechanism of Ruthenium-Catalyzed Hydrogen Transfer Reactions. Concerted Transfer of OH and CH Hydrogens from an Alcohol to a (Cyclopentadienone)ruthenium Complex. *J. Org. Chem.* **2003**, *68*, 7681–7684. (d) Dub, P. A.; Gordon, J. C. The mechanism of enantioselective ketone reduction with Noyori and Noyori–Ikariya bifunctional catalysts. *Dalton Trans.* **2016**, *45*, 6756–6781. (e) Dub, P. A.; Gordon, J. C. Metal–Ligand Bifunctional Catalysis: The “Accepted” Mechanism, the Issue of Concertedness, and the Function of the Ligand in Catalytic Cycles Involving Hydrogen Atoms. *ACS Catal.* **2017**, *7*, 6635–6655.

(20) For oxidative formation of amide-bond containing pharmaceuticals from corresponding alcohol and amine, see: Piszal, P. E.; Vasilopoulos, A.; Stahl, S. S. Oxidative Amide Coupling from Functionally Diverse Alcohols and Amines Using Aerobic Copper/Nitroxyl Catalysis. *Angew. Chem., Int. Ed.* **2019**, *58*, 12211–12215.

(21) Moclobemide. In *Meyler’s Side Effects of Drugs*, 16th ed.; Aronson, J. K., Ed.; Elsevier: Oxford, 2016; pp 1076–1080.

(22) (a) For other alternative methods to synthesize moclobemide, see: Singha, K.; Ghosh, S. C.; Panda, A. B. N-Doped Yellow TiO<sub>2</sub> Hollow Sphere-Mediated Visible-Light-Driven Efficient Esterification of Alcohol and N-Hydroxyimides to Active Esters. *Chem.—Asian J.* **2019**, *14*, 3205–3212. (b) Bantreil, X.; Kanfar, N.; Gehin, N.; Golliard, E.; Ohlmann, P.; Martinez, J.; Lamaty, F. Iron-catalyzed benzamide formation. Application to the synthesis of moclobemide. *Tetrahedron* **2014**, *70*, 5093–5099.

(23) <https://www.drugbank.ca/drugs/DB04924> (accessed Feb 06, 2021).